

Equilibrium and nonequilibrium molecular dynamics methods to compute the first normal stress coefficient of a model polymer solution

A. G. Menzel and P. J. Daivis^{✉*}*School of Science, RMIT University, GPO Box 2476, Melbourne, Victoria, 3001, Australia*B. D. Todd[✉]*Department of Mathematics, Faculty of Science, Engineering and Technology, Swinburne University of Technology, P.O. Box 218, Hawthorn, Victoria, 3122, Australia*

(Received 25 October 2019; accepted 16 July 2020; published 14 August 2020)

The zero-shear first normal stress coefficient, $\Psi_{1,0}$, is an important viscometric function used throughout rheology. It can be directly computed by using various molecular dynamics simulation methods. Homogeneous shear algorithms used in nonequilibrium molecular dynamics simulations require some type of synthetic thermostat to remove dissipated heat resulting from the work done by the shear. While it has been shown conclusively that the linear transport coefficients are unaffected by synthetic thermostats, some doubt remains for the first normal stress coefficient. This problem can be circumvented by performing inhomogeneous Poiseuille flow simulations where heat is removed by thermal conduction to thermostatted walls. Alternatively, we can use equilibrium computations to calculate the properties of interest. This is significantly more difficult for nonlinear properties than it is for the linear transport properties. Here we present three different methods of calculating the first normal stress coefficient for a model polymer solution; in one, the computations are performed in equilibrium conditions (Coleman-Markovitz equation) and in the other two they are carried out in nonequilibrium conditions (SLLOD and Poiseuille flow). We find that both nonequilibrium methods produce matching results, with $\Psi_{1,0} = 170 \pm 2$ for SLLOD and $\Psi_{1,0} = 172 \pm 3$ for Poiseuille flow, regardless of whether the fluid of interest is directly or indirectly thermostatted. The Coleman-Markovitz result is difficult to resolve, and much less accurate, with $\Psi_{1,0} \approx 190$, although it still may not be fully converged, even after extensive computations. We suggest that the Coleman-Markovitz equation is unsuitable for routine determination of the first normal stress coefficient by molecular simulation.

DOI: [10.1103/PhysRevFluids.5.084201](https://doi.org/10.1103/PhysRevFluids.5.084201)

I. INTRODUCTION

Normal stress differences are related to the viscoelasticity of a material and have long been used to characterize various aspects of polymer rheology. They are important in microfluidics [1], the structure of vortices [2], and even in shock-wave mechanics [3]. Nonequilibrium molecular dynamics (NEMD) simulations can be a powerful tool to investigate these phenomena, however previous work [4–6] has suggested that the choice of thermostat used in homogeneous shear NEMD simulations might affect the first normal stress coefficient, $\Psi_{1,0}$, and possibly even any property that varies with the square of the strain rate, potentially leading to incorrect results. Daivis *et al.* [5] have shown that the SLLOD method of obtaining $\Psi_{1,0}$ produced a value half that of the value obtained

*peter.daivis@rmit.edu.au

using the Coleman-Markovitz equation [7] for a simple atomic fluid with very small normal stress differences. Furthermore, some choices of thermostating strategy for the SLLOD simulations also changed the calculated value of $\Psi_{1,0}$.

In this study we investigate normal stress effects for a model polymer solution with significant normal stress differences. In one set of simulations, we subject this system to planar Poiseuille flow driven by body forces of various strengths. In these simulations, we implement a novel method of calculating the first normal stress coefficient. This new method involves computing the individual components of the pressure tensor locally—allowing the calculation of the first normal stress coefficient as a function of position (and therefore strain rate) in the channel. In this system, the confined fluid is naturally thermostatted via its interactions with the wall. We compare our calculated value of the limiting zero shear rate first normal stress coefficient with the values obtained from both thermostatted homogeneous shear NEMD simulations using the SLLOD algorithm and equilibrium molecular dynamics (EMD) simulations using the Coleman-Markovitz equation. This allows us to critically evaluate previous research that suggests that synthetic thermostats can interfere with various fluid properties.

II. SIMULATION METHOD AND THEORY

For this study we used a molecular dynamics (MD) code produced in-house which implements algorithms described elsewhere [8]. This code solves for the position and momentum of every particle in the system, explicitly including solvent particles, using Newtonian equations of motion.

All particles in this work are simulated with equal mass m and pairwise interactions are computed using the Weeks-Chandler-Anderson (WCA) potential [9] which is a purely repulsive, truncated and shifted version of the Lennard-Jones (LJ) pair potential, given as

$$\phi_{\text{WCA}}(r) = \begin{cases} \phi_{\text{LJ}}(r) + \epsilon & r < 2^{1/6}\sigma \\ 0 & r \geq 2^{1/6}\sigma \end{cases} \quad (1)$$

where

$$\phi_{\text{LJ}}(r) = 4\epsilon \left[\left(\frac{\sigma}{r} \right)^{12} - \left(\frac{\sigma}{r} \right)^6 \right], \quad (2)$$

ϵ is the depth of the potential energy well, σ is the interatomic separation at which the LJ potential is zero, and r is the pair separation distance. Simulation parameters and results are given in reduced units based on the characteristic length scale, σ , and energy scale, ϵ , of this potential and the reduced mass scale m of the individual particles. The equations of motion for every system in this work are solved using a fifth-order Gear-predictor-corrector algorithm [10] with a reduced timestep of $\delta t = 0.001$.

In this paper we present results for the first normal stress coefficient of a model polymer solution obtained by three different methods. The first two methods involve simulations of the polymer solution under homogeneous conditions with periodic boundary conditions in all three directions. Both equilibrium and nonequilibrium molecular dynamics simulations are performed for the homogeneous systems. In both of these cases, the fluid is directly thermostatted using a synthetic homogeneous thermostat incorporated into the equations of motion. The last method simulates the polymeric fluid under confinement between two planar walls. An external field is applied to generate Poiseuille flow. In this case, the fluid is not directly thermostatted, but heat generated in the fluid is conducted through the fluid to the walls where it is removed by a synthetic thermostat. Each of the simulation methods used is described in the following sections.

TABLE I. Overview of system parameters. EQ-GK refers to the equilibrium Green-Kubo system, NE-SL refers to the nonequilibrium SLLD system, and NE-PF refers to the nonequilibrium Poiseuille flow system. T is the set temperature for the thermostat, ρ is the nominal mass density, L_α is the length of the undeformed simulation box in direction α . Finally, N_β is the number of atoms in the wall w , polymers p , and solvent s , and N_{pm} is the number of polymer molecules.

System	T	ρ_f	L_x	L_y	L_z	N_w	N_p	N_s	N_{pm}
EQ-GK	1.0163	0.841	22.82	22.82	18.26	0	1600	6400	80
NE-SL	1.01	0.841	22.82	22.82	18.26	0	1600	6400	80
NE-PF	1	0.840	20.98	86.66	5.74	456	1680	6720	84

A. Homogeneous methods

1. First normal stress coefficient from equilibrium

The homogeneous system studied here consists of 80 20-site freely jointed polymer chains in a solution of 6400 solvent atoms. The mass of a polymer molecule is 20 in reduced mass units with each site having a reduced mass of 1. The reduced mass of each solvent atom is also 1. This is identical to the model polymer solution studied by Kairn *et al.* [11] who pointed out that this model polymer is equivalent to polyethylene of molar mass approximately equal to 1800 g/mol. Thus, this is a very short chain polymer and consequently the shear rate dependent behavior that we report is only observed at shear rates that are much higher than experimentally attainable values. The concentration of the polymer species is given by $c_1 = \rho_1/(\rho_1 + \rho_2) = 0.20$, where ρ_α is the mass density of species α , 1 refers to the polymer species, and 2 to the solvent. Because the masses of the polymer sites and solvent atoms are all equal to unity, the mass density is identical to the number density. As such, this concentration can be considered as either a ‘‘mass’’ or ‘‘number’’ fraction.

The total fluid density in the simulation box is $\rho = 0.841$ with the simulation box lengths $L_x = L_y \approx 22.82$ and $L_z \approx 18.26$. This value of the density was chosen to match the value of the channel center density in the Poiseuille flow system described in the following section.

An overview of this system’s properties can be found in Table I.

This system was simulated at equilibrium, with thermostatted Newtonian equations of motion,

$$\dot{\mathbf{r}}_{i\alpha} = \frac{\mathbf{p}_{i\alpha}}{m}, \quad (3)$$

and

$$\dot{\mathbf{p}}_{i\alpha} = \mathbf{F}_{i\alpha}^\phi + \mathbf{F}_{i\alpha}^C - \xi \mathbf{p}_i, \quad (4)$$

where the subscripts $i\alpha$ refer to the α th particle on the i th molecule, $\dot{\mathbf{r}}$ is the velocity, \mathbf{p} is the momentum, m is the mass, which is identical for each particle, \mathbf{F}^ϕ is the sum of forces due to interatomic potentials on the particle, given by the spatial derivative of Eq. (1), \mathbf{F}^C is the sum of constraint forces on the particle, which is zero for solvent particles, and otherwise evaluated using the Gaussian constraint algorithm [8], and $\mathbf{p}_i = \sum_\alpha \mathbf{p}_{i\alpha}$, which is the molecular center of mass momentum. Finally, ξ is the Gaussian Isokinetic thermostat multiplier, given by

$$\xi = \frac{\sum_i \mathbf{p}_i \cdot \mathbf{F}_i / M_i}{\sum_i \mathbf{p}_i^2 / M_i}, \quad (5)$$

where $\mathbf{F}_i = \sum_\alpha (\mathbf{F}_{i\alpha}^\phi + \mathbf{F}_{i\alpha}^C)$ and M_i is the mass of molecule i , $M = 20$ for polymer molecules, and $M = 1$ for solvent molecules.

In this equilibrium homogeneous system we can calculate the first normal stress coefficient using the Coleman-Markovitz equation [7], which is a Green-Kubo-like integral of a correlation function given by [12]

$$\Psi_{1,0} = \frac{V}{5k_B T} \int_0^\infty \tau \langle \mathbf{P}^{\text{ts}}(0) : \mathbf{P}^{\text{ts}}(\tau) \rangle d\tau \quad (6)$$

$$= 2 \int_0^\infty \tau G(\tau) d\tau, \quad (7)$$

where k_B is Boltzmann's constant, T is the temperature, τ is the delay time of the correlation function, $G(\tau)$ is the shear relaxation modulus, and $\mathbf{P}^{\text{ts}} = (\mathbf{P} + \mathbf{P}^T)/2 - \text{Tr}(\mathbf{P})\mathbf{I}/3$ is the traceless-symmetric part of the pressure tensor.

2. First normal stress coefficient from homogeneous shear

The first normal stress coefficient can also be obtained by simulating a homogeneous system experiencing a constant shear-rate deformation. The algorithm we used is the SLLOD equations of motion [8] given by

$$\dot{\mathbf{r}}_{i\alpha} = \frac{\mathbf{p}_{i\alpha}}{m_{i\alpha}} + \mathbf{r}_i \cdot \nabla \mathbf{v}, \quad (8)$$

and

$$\dot{\mathbf{p}}_{i\alpha} = \mathbf{F}_{i\alpha} - \frac{m_{i\alpha}}{M_i} \mathbf{p}_i \cdot \nabla \mathbf{v} - \xi \frac{m_{i\alpha}}{M_i} \mathbf{p}_i, \quad (9)$$

where \mathbf{p} in these equations refers to the thermal (also ‘‘peculiar’’) momentum, \mathbf{v} is a velocity field applied to the molecular center of mass, M_i is the molecular mass, and \mathbf{F} is the sum of the interatomic and constraint forces on the particle.

The system used for the SLLOD simulations is chosen to have the same state point as for the equilibrium simulation described previously. This system has 80 polymer molecules and 6400 solvent molecules, for a total of 8000 atoms at a mass concentration of $c_1 = 0.20$. The size of the simulation box is $L_x = L_y = 22.82$ and $L_z = 18.26$ giving a total mass density of $\rho = 0.841$, chosen to match the center channel density of the Poiseuille flow system at equilibrium, which is slightly different from the average density due to atomic packing and depletion effects close to the walls. For these equations of motion the molecular center-of-mass Gaussian isokinetic thermostat given by Eq. (5) must be modified to account for the imposed flow:

$$\xi = \frac{\sum_i \mathbf{p}_i \cdot (\mathbf{F}_i - \mathbf{p}_i \cdot \nabla \mathbf{v}) / M_i}{\sum_i \mathbf{p}_i^2 / M_i}. \quad (10)$$

The set temperature of the thermostat applied to the entire fluid is 1.01, chosen to be similar to the maximum temperature observed in the Poiseuille flow simulations described in the next section.

We can then calculate the first normal stress coefficient directly, at a particular value of the strain rate. In this system, flow is generated in the x direction with a velocity gradient in the y direction, and under this convention we have

$$\Psi_1(\dot{\gamma}) = \frac{P_{yy} - P_{xx}}{\dot{\gamma}^2}, \quad (11)$$

where $P_{\alpha\alpha}$ is a normal component of the pressure tensor and $\dot{\gamma}$ is the strain rate.

After obtaining this value for various strain rates within a sufficiently narrow range near zero strain rate, we fit the data with a quadratic function (since the first normal stress difference should be an even function of the strain rate due to symmetry) and extrapolate Ψ_1 back to the zero strain rate value, $\Psi_{1,0}$ to compare with the zero strain rate value calculated in equilibrium via Eq. (6).

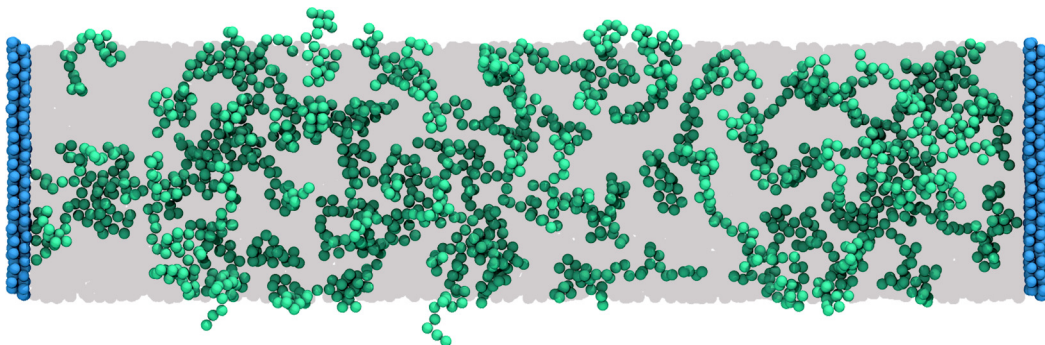


FIG. 1. Visualization of the simulated system. The explicit solvent atoms have been displayed as a grayed out continuum for clarity. The polymer is shown in green and the walls are shown in blue. In this image, the x direction is vertical, the y direction horizontal, and the z direction in and out of the page.

B. Poiseuille flow method

The confined system presented here is a two component fluid consisting of 84 20-site freely jointed polymer molecules in a solution of 6720 solvent atoms. Each polymer molecule has a total reduced mass of 20, 1 reduced mass unit for each of the 20 sites in the chain, and the solvent sites each have a reduced mass of 1. The solution has an average polymer mass fraction concentration of $c_1 = 0.2$. The average fluid mass (and site number) density is $\rho = 0.84$. Due to polymer depletion and fluid packing near the walls, the center channel values differ slightly from the average values. The fluid is confined in the y direction on both sides by a 2 layered Hexagonal-Close-Packed wall, consisting of 228 atoms each at a nominal mass density of 1.05, and separated by approximately 86.6 reduced length units. This box shape was chosen to provide a sufficiently wide center channel region where the fluid velocity and the pressure tensor components were well described by polynomial fits [13]. The system has periodic boundary conditions in the x direction (the flow direction) and the z direction, effectively simulating an infinite slab of fluid between two infinite plates. A visualisation of this system can be found in Fig. 1. All systems were run for at least 2×10^7 timesteps (20 000 reduced time units) to allow the steady state to be established before accumulating averages. An overview of the system properties can be found in Table I.

The equations of motion for all fluid particles are as follows:

$$\dot{\mathbf{r}}_{i\alpha} = \frac{\mathbf{p}_{i\alpha}}{m} \quad (12)$$

and

$$\dot{\mathbf{p}}_{i\alpha} = \mathbf{F}_{i\alpha}^{\phi} + \mathbf{F}_{i\alpha}^{\text{C}} + m\mathbf{F}^{\text{e}}. \quad (13)$$

In these equations the subscript $i\alpha$ refers to the α th atom on the i th molecule, $m\mathbf{F}^{\text{e}}$ is the gravity-like body force applied to fluid particles to induce Poiseuille flow.

The equations of motion for the walls are

$$\dot{\mathbf{r}}_i = \frac{\mathbf{p}_i}{m} \quad (14)$$

and

$$\dot{\mathbf{p}}_i = \mathbf{F}_i^{\phi} + \mathbf{F}_i^{\text{W}} - \alpha_{\beta}\mathbf{p}_i + \lambda_{\beta}\hat{\mathbf{y}}, \quad (15)$$

where $\mathbf{F}_i^{\text{W}} = -k(\mathbf{r}_i - \mathbf{r}_i^{\text{eq}})$ is a harmonic tethering force used to tether the wall particles to their equilibrium positions, \mathbf{r}_i^{eq} , with $k = 57.15$, which has been determined to work well for this system [14]. α_{β} is a Gaussian isokinetic thermostat multiplier applied to the β th layer, and λ_{β} is a center of

mass constraint applied to the β th layer to stop the layers from moving in response to the normal pressure exerted on the walls by the fluid [8].

It is important to note that the equations of motion for the fluid given by Eqs. (12) and (13) do not include a synthetic thermostat, while the equations of motions for the walls do. The fluid temperature in this system is naturally controlled by heat conduction to the thermostatted walls, where it is removed by a synthetic thermostat.

To calculate the pressure locally we use the volume averaged form of the pressure tensor, originally developed by Cormier *et al.* [15],

$$\begin{aligned} \mathbf{P}_{\text{VA}}(\mathbf{r}) = & \frac{1}{\delta V} \left(\sum_i \sum_{\alpha} m \mathbf{c}_{i\alpha} \mathbf{c}_{i\alpha} \Lambda_{i\alpha} \right. \\ & - \frac{1}{2} \sum_i \sum_j \sum_{\alpha} \sum_{\beta}^{\dagger} \mathbf{r}_{i\alpha, j\beta} \mathbf{F}_{i\alpha, j\beta}^{\phi} l_{i\alpha, j\beta} \\ & \left. - \frac{1}{2} \sum_i \sum_{\alpha} \sum_{\beta=\alpha\pm 1} \mathbf{r}_{i\alpha, i\beta} \mathbf{F}_{i\alpha, i\beta}^{\text{C}} l_{i\alpha, i\beta} \right), \end{aligned} \quad (16)$$

which we have modified to include the contribution due to the constraint forces on the atoms within the polymer molecules. Here the subscripts α and β refer to particle indices on molecules i and j , respectively. δV is the volume element under consideration, \mathbf{c}_i is the peculiar velocity vector, m is the mass, $\Lambda_{i\alpha}$ is a selection function equal to 1 when the particle is inside the volume element and 0 otherwise, $\mathbf{r}_{i\alpha, j\beta}$ is the separation vector between particle pairs, $\mathbf{F}_{i\alpha, j\beta}^{\phi}$ is the force due to the interatomic potential on site $i\alpha$ due to site $j\beta$, $\mathbf{F}_{i\alpha, j\beta}^{\text{C}}$ is the constraint force on site $i\alpha$ due to site $j\beta$ and $l_{i\alpha, j\beta}$ is the fraction of the length of the separation vector that falls within the averaging volume. Finally, the daggered sum in the second term is a restricted sum over β that excludes both self pair forces and those between adjacent atoms on the same molecule. In total the first term represents the kinetic contribution to the pressure tensor, the second represents the configurational contribution due to the pair forces, and the third represents the configurational contribution due to the intramolecular constraints. This pressure is an ‘‘atomic pressure,’’ meaning the forces are localized on the atomic and not the molecular centers of mass.

Heyes *et al.* [16] have demonstrated the equivalence of the volume averaged form of the pressure tensor presented in Eq. (16) to the method of planes from Todd *et al.* [17] in the limit of $\delta V \rightarrow 0$. The volume averaged form gives an accurate representation of the local pressure tensor components even when strong inhomogeneity exists, provided that the bins over which the averaging is performed are sufficiently narrow. A similar approach has recently been used to calculate the local volume averaged heat flux vector in a highly inhomogeneous fluid [18].

In order to calculate the local pressure tensor components accurately, we split the channel up into 400 equally sized averaging volumes (bins) in the y direction, perpendicular to the walls. The volume averaged pressure tensor is then calculated for each of these bins, accumulated every 20 timesteps and averaged over 3×10^8 timesteps across an ensemble of 16 statistically independent instances of the system for an effective total reduced sampling time of 5×10^5 . Since the volume is only divided in a single direction, we use a simple geometric argument to calculate the value of l_{ij} .

By using the following equation we can calculate the first normal stress coefficient as a function of position across the channel:

$$\Psi_1(y) = \frac{P_{yy}(y) - P_{xx}(y)}{\dot{\gamma}^2(y)}, \quad (17)$$

where $P_{\alpha\alpha}(y)$ are the corresponding normal components of the local pressure tensor evaluated locally and $\dot{\gamma}(y)$ is the local strain rate, calculated by numerical differentiation of the velocity profile.

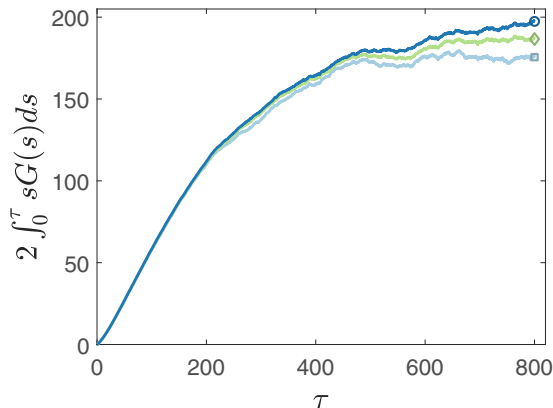


FIG. 2. The cumulative integral of the first moment of the stress autocorrelation function. Converged values correspond to the first normal stress coefficient, $\Psi_{1,0}$, given by Eq. (6). Each line corresponds to a different value of the total averaging time, where the symbol terminating the line corresponds to the following values of the averaging time: $t_{\text{av}}^{\square} = 4 \times 10^7$, $t_{\text{av}}^{\diamond} = 6 \times 10^7$, and $t_{\text{av}}^{\circ} = 8 \times 10^7$.

III. RESULTS AND DISCUSSION

First, we present the EMD Coleman-Markovitz results for the homogeneous system. Figure 2 shows the cumulative integral of the first moment of the stress autocorrelation function [given by Eq. (6)] over a delay time of 800 reduced time units for 3 different values of the total averaging time. The stress correlation function $G(\tau)$ was sampled every 10 timesteps (every 0.01 time units), and had 80 000 shift registers. It was also averaged over 96 separate instances of the system, each prepared with a different initial state. In total the simulation was run for the equivalent of more than 8×10^{10} timesteps in the preparation of this plot. The stress autocorrelation function for this system is very slowly relaxing. When it is multiplied by the delay time, giving the first moment, as in Eq. (6), convergence of its integral is very difficult to obtain.

Figure 2 shows that comparatively early in the averaging process the integral looks converged with $\Psi_{1,0} \approx 170$ at $t_{\text{av}} = 4 \times 10^7$; however, with twice as much averaging time $t_{\text{av}} = 8 \times 10^7$ we have seemingly $\Psi_{1,0} \approx 190$. It is difficult to discern whether the integral simply remains noisy, or fails to converge.

The Coleman-Markovitz integral converges slowly because the shear relaxation modulus $G(\tau)$ is already a slowly decaying function (usually modelled as a distribution of exponential relaxations for polymeric materials) and it is multiplied by τ before being integrated. In principle, this integral should nevertheless eventually converge. The convergence of the Coleman-Markovitz integral is problematic, even for simple liquids. If the asymptotic decay of the stress autocorrelation function is exponential as predicted by the Boltzmann and Enskog equations [19], then the Coleman-Markovitz integral must converge. However, mode-coupling theory calculations have shown that the stress relaxation function for a simple liquid in 3 dimensions is expected to decay as $\tau^{-3/2}$. In that case, the integrand goes as $\tau^{-1/2}$, which when integrated increases as $\tau^{1/2}$ instead of approaching a constant value in the infinite time limit. Such behavior would imply that the first normal stress coefficient calculated from the Coleman-Markovitz equation does not exist for simple liquids. Experiments clearly show that it is possible to measure the first normal stress coefficient, so its existence is not in question. The Coleman-Markovitz result can be obtained from a variety of single integral, finite viscoelastic continuum models of polymer rheology [20] but the generality of the Coleman-Markovitz equation for all materials and timescales and the precise nature of the long time decay of the stress autocorrelation function are both yet to be fully understood. Molecular dynamics results for simple liquids show considerable complexity in the long time decay of the stress autocorrelation

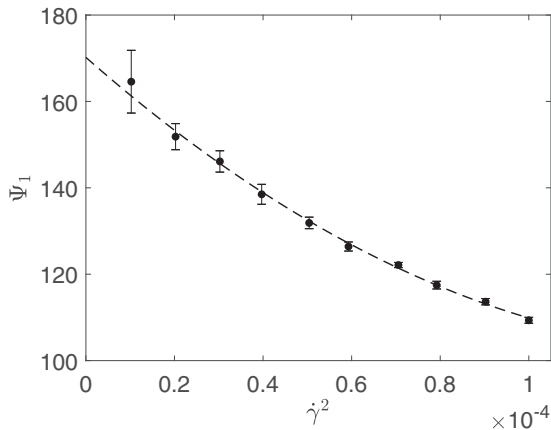


FIG. 3. Value of the first normal stress coefficient as a function of shear rate, calculated from SLLOD simulations and Eq. (11). The dashed line shows a quadratic fit to the data.

function, including a slowly-decaying “molasses tail” at high densities with an algebraic $\tau^{-3/2}$ decay similar to that predicted by mode-coupling theory. The predicted $\tau^{-3/2}$ tail is not observed for all materials or under all conditions and its amplitude is sometimes much greater than predicted by mode-coupling theory, which may indicate that it is possibly the molasses tail that is observed rather than the hydrodynamic tail predicted by mode-coupling theory [21]. Thus, there remains considerable doubt that the algebraic tail predicted by mode-coupling theory is always observed in simulations of simple liquids.

Assuming the integral does converge in our case, the gradient in the largest averaging time integral suggests that convergence may occur at yet higher maximum delay times. Ultimately, it is not clear whether the integral converges, for our system specifically, nor in the general case of molecular simulations. Furthermore when convergence has been seen in the literature the value found for the normal stress coefficient from the Coleman-Markovitz equation disagrees with those found through other methods [5].

Figure 2 was produced from 300 000 CPU hours of simulation on a high performance computing cluster. By further doubling the averaging time, and/or doubling the maximum delay time for the correlation function, it may be possible to resolve this issue; however, that is beyond the capacity of this study.

Ultimately the Coleman-Markovitz equation approach is unsuited to evaluating the first normal stress coefficient in simulations of molecular systems, and especially those which are slowly relaxing. In this case our simulations are relatively cheap, and our polymer chain lengths comparatively small. Complex potentials, long polymer chains and higher concentrations would each compound the difficulties of evaluating the Coleman-Markovitz equation further.

Figure 3 shows the results of homogeneous shear computations of the first normal stress coefficient using the SLLOD algorithm. The shear rate dependencies of the viscosity and normal stress coefficients for polymeric liquids are usually described by power laws. These properties are observed to become more weakly dependent on strain rate as the zero shear rate limit is approached. Nonequilibrium molecular dynamics simulation data for alkanes, short chain polymers and molecular liquids all display polynomial dependence on the strain rate in the low strain rate limit. It has been shown that the best agreement between the viscosity computed using the equilibrium Green-Kubo formula (which necessarily gives the zero shear rate viscosity) and the shear rate dependent viscosity from nonequilibrium molecular dynamics is found by using a polynomial fitting function in the very low shear rate regime [8,22]. Extrapolation of a quadratic fit to the data for $\Psi_1(\dot{\gamma})$ to zero strain rate gave the value of the zero shear rate normal stress coefficient

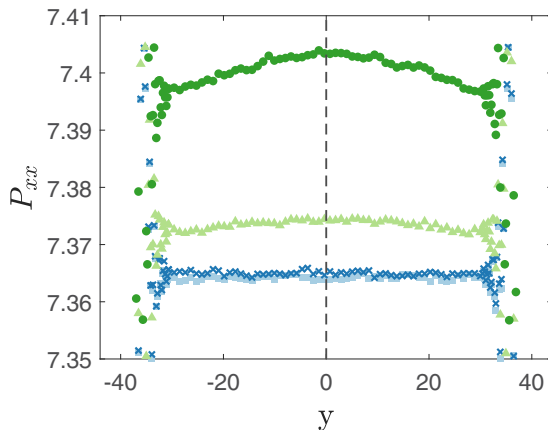


FIG. 4. The value of P_{xx} across the channel for body forces of $F^e = 10^{-3}$ (circles), 5×10^{-4} (diamonds), 10^{-4} (crosses), 0 (squares). Some data points have been omitted for visual clarity.

as $\Psi_{1,0} = 170 \pm 2$. The viscosity of this system was previously reported [13] as $\eta = 3.69$, which agrees well with the earlier result of $\eta = 3.64$ from a fit to the concentration dependence of the viscosity by Kairn *et al.* [11]. For comparison, the viscosity of this system at zero polymer concentration is 1.9 ± 0.1 [11]. The first normal stress data of Kairn *et al.* are unfortunately too noisy for a reliable comparison.

It is important to remember that the SLLOD method of simulation requires the fluid to be thermostatted, which in principle could affect the value of $\Psi_{1,0}$ as found previously for an atomic fluid [5]. The SLLOD value is close to the values given by the Coleman-Markovitz equation. However, since the convergence of the Coleman-Markovitz integral is uncertain this cannot act as a check against the thermostatted SLLOD method. We must rely on the results from the Poiseuille flow system to act as a check on the SLLOD method, and to determine what effect, if any, the synthetic thermostat has on the first normal stress coefficient.

For our Poiseuille flow system, we first present the results for the local pressures across the channel. Figure 4 shows the variation of P_{xx} across the channel for different values of the body force. As the body force used to produce Poiseuille flow increases, the value and the curvature of P_{xx} both increase. The large spread in data points towards the sides is a result of large density variations in the fluid due to packing effects near the walls, rather than statistical noise. The local pressure is incredibly sensitive to even small variations in the density.

In our previous paper [13], we discussed the density, velocity, temperature, and concentration profiles of the polymer solution at equilibrium and in planar Poiseuille flow. These results showed small but measurable slip at the walls in Poiseuille flow, and strong depletion effects at equilibrium and under flow due to the entropy penalty associated with conformations in which the polymer molecules must be distorted from their preferred random coil conformation to closely approach the wall. Normal pressure data from the regions nearest the walls where depletion effects were present were omitted from the analysis. At the very low values of the external driving field employed here, our previous work has shown that the temperature variation across the channel is negligible and the concentration variation is also very weak outside the depletion region [13].

Figure 5 shows P_{yy} as a function of position across the channel. The absolute value of P_{yy} changes with body force, but it remains independent of position. This is expected since the confining presence of the walls entails a momentum balance in the constrained direction, giving $\frac{dP_{yy}}{dy} = 0$. Note that the magnitudes of the normal pressures, P_{xx} and P_{yy} , match at the channel center, where the shear-rate (shown in Fig. 7) is zero. This is expected since the zero shear bin essentially corresponds

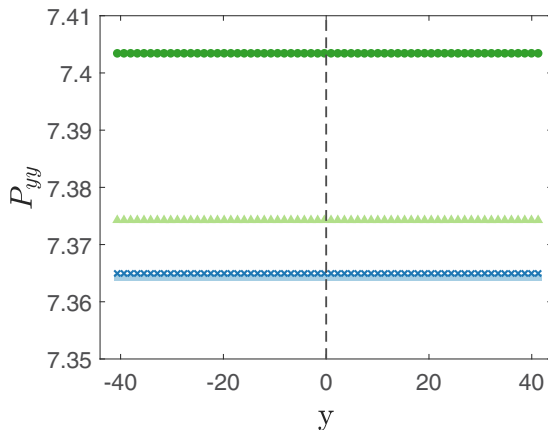


FIG. 5. The value of P_{yy} across the channel for body forces of $F^e = 10^{-3}$ (circles), 5×10^{-4} (diamonds), 10^{-4} (crosses), 0 (squares). Some data points have been omitted for visual clarity.

to a local equilibrium system with $\dot{\gamma} = 0$ where the normal pressure components are expected to be identical.

Figure 6 shows the value of $N_1 = P_{yy} - P_{xx}$ across the channel for each body force. The dashed line gives a fit to the data of the form

$$N_1(y) = n_2y^2 + n_4y^4, \quad (18)$$

resulting in a quadratic coefficient of $7.78(21) \times 10^{-9}$, $2.22(20) \times 10^{-6}$, and $9.66(21) \times 10^{-6}$ for body forces $F^e = 0.0001$, 0.0005 , and 0.001 , respectively. The quartic coefficients for the respective body forces are $7(20) \times 10^{-11}$, $5(2) \times 10^{-10}$, $-1.90(23) \times 10^{-9}$. Note that the figures indicated in brackets constitute uncertainties in the final digits listed.

Figure 7 shows the value of the local strain rate across the channel for each body force. The dotted line gives a fit to the data of the form

$$\dot{\gamma}(y) = g_1y + g_2y^2, \quad (19)$$

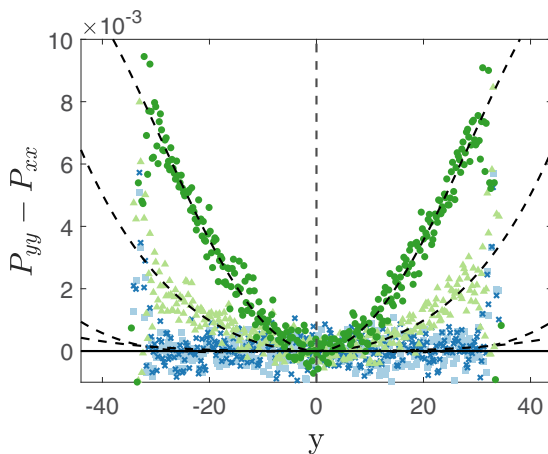


FIG. 6. The value of $P_{yy} - P_{xx}$ across the channel for body forces of $F^e = 10^{-3}$ (circles), 5×10^{-4} (diamonds), 10^{-4} (crosses), 0 (squares).

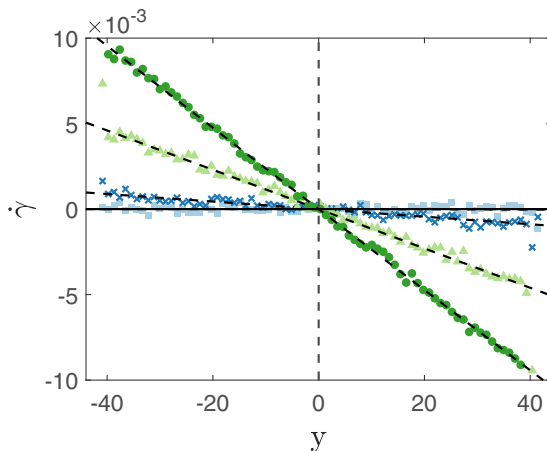


FIG. 7. The value of $\dot{\gamma}$ across the channel for a body forces of $F^e = 10^{-3}$ (circles), 5×10^{-4} (triangles), 10^{-4} (crosses), 0 (squares). Some data points have been omitted for visual clarity.

resulting in a linear coefficient of $-2.21(5) \times 10^{-5}$, $-1.15(1) \times 10^{-4}$, and $-2.37(1) \times 10^{-4}$ for body forces $F^e = 0.0001$, 0.0005 , and 0.001 , respectively. The quadratic coefficients for the respective body forces, were $-5(200) \times 10^{-10}$, $-3(200) \times 10^{-10}$, $4(2) \times 10^{-8}$. Thus, the deviations from a linear strain rate profile over the range of the fits were less than the uncertainties for the two lowest values of the body force.

The forms of Eqs. (18) and (19) were chosen to account for the possibility of a nonlinear shear response. The values obtained indicate that the nonlinear response is small enough for the normal pressure components to be well described by a fourth order polynomial function. This is consistent with the SLLOD data where the maximum reduced strain rate studied was 10^{-2} , which compares well with the maximum strain rate at the sides of the channel which can be seen in Fig. 7.

We can evaluate the first normal stress coefficient for this system by substituting the fitted equations into the expression for the first normal stress coefficient given by Eq. (17) and taking the zero shear rate (zero y) limit.

This gives us the following equation:

$$\Psi_{1,0} = \frac{n_2}{(g_1)^2}. \quad (20)$$

Here, we have assumed that only the quadratic and linear components of Eqs. (18) and (19), respectively, contribute to the zero-shear rate limit of the response of the normal pressure.

By substituting the fitted coefficients into this equation we obtain three different estimates for the first normal stress coefficient in our confined polymer solution system, shown in Fig. 8. The dashed line gives the value of the first normal stress coefficient obtained from the thermostatted SLLOD method, from Eq. (11), $\Psi_{1,0} = 170 \pm 2$, which can be seen in Fig. 3.

The uncertainties in the values are large due to the small body forces and the resulting small gradient in the local normal stress difference, however agreement with the SLLOD value is very good, particularly for the body forces which produce a significant response in the pressure tensor. For body forces $F^e = 0.0001$, 0.0005 , and 0.001 , the values are $\Psi_{1,0} = 159 \pm 420$, 169 ± 13 , and 172 ± 3 , respectively.

Agreement between the SLLOD and Poiseuille flow values indicates that the SLLOD values, where the total thermal kinetic energy is thermostatted, are correct. However, Daivis *et al.* [5] observed that the normal stress coefficient varied when different types of thermostat were applied. Closer inspection of the data reported by Daivis *et al.* [5] shows that the discrepancies only occurred between SLLOD systems with and without an over-constrained kinetic temperature, where

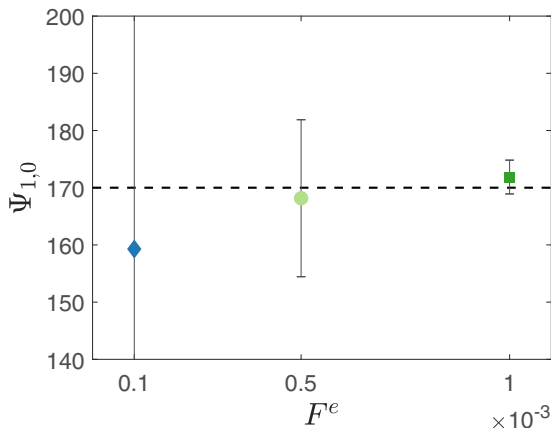


FIG. 8. Values of the first normal stress coefficient calculated from Eq. (11) for body forces of $F^e = 10^{-3}$, 5×10^{-4} , and 10^{-4} . The dotted line gives the value of the first normal stress coefficient extracted from Fig. 3.

$K_x \equiv K_y \equiv K_z$. This directly corresponds to completely constraining the kinetic term of the pressure. Complete constraint of the directional configurational temperatures, however, does not completely constrain the configurational term in the pressure. In our case, only the total kinetic temperature is constrained, which allows the directional components to fluctuate as normal.

Although it was overlooked by Davis *et al.* [5], this is to be expected. Evans and Sarman [23] have shown that the Gaussian isoenergetic and Gaussian isokinetic thermostatted nonlinear responses are identical in the steady state only if the phase variable in question has no trivial relationship to the constants of motion. In the case of our SLLOD simulations, constraint of the total kinetic energy has no trivial relationship to the normal pressures. But constraining each directional kinetic temperature would create a trivial relationship between each normal pressure and its corresponding directional temperature. This indicates that only when completely constraining the directional kinetic energy, or any other trivially related variable, will the thermostatted response of the pressure differ from other nontrivially thermostatted and unthermostatted responses.

Davis *et al.* [5] showed that evaluation of the first normal stress coefficient from the Coleman-Markovitz relation gave a result that was approximately a factor of two larger than the SLLOD value for a simple WCA fluid. We have repeated these simulations and found the same result. We suggest that, in light of this new data, it is possible that the Coleman-Markovitz integral leads to an incorrect value of the first normal stress coefficient in some simulated systems, even when converged. This could be due to the failure of one of the assumptions made in deriving the “second order fluid” model from which the Coleman-Markovitz equation is obtained [7]. Coleman and Markovitz assume that the extra stress is a functional of the symmetric strain tensor. They then assume that the history can be expanded about the present time as a Taylor series using the material derivatives of the strain history. This corresponds to the “slow flow” approximation in which it is assumed that the deformation relative to the current configuration over the recent past (determined by the decay of an influence function which is essentially a memory kernel) is small. We note that the main mechanisms responsible for the first normal stress difference in atomic and polymeric fluids are different. For an atomic fluid it is distortion of the radial distribution function and for a polymeric fluid it is chain stretching and alignment, so that much higher strain rates are required to observe normal stress differences in simple atomic fluids than for polymeric fluids. These differences may mean that the extent to which the assumptions are satisfied is different for the two fluids. Furthermore, while convergence of the Coleman-Markovitz integral has been shown for atomic systems [5,21], it is still unknown whether or not it converges in the much more slowly relaxing polymer fluid case presented here.

Our previous work [13] on the model polymer solution discussed here gives the value for the viscosity as $\eta = 3.69$. We found excellent agreement between the viscosity calculated from the integral of the equilibrium shear relaxation modulus $G(\tau)$ using the Green-Kubo relation and the results from nonequilibrium SLLOD and Poiseuille flow simulations. This confirms that our calculation of the shear relaxation modulus is reliable. Combining this viscosity result with our first normal stress coefficient value of $\Psi_{1,0} = 170$ we find a relaxation time for the shear relaxation modulus of $\tau_s = \Psi_{1,0}/(2\eta) = 23$. In the case of a short chain polymer melt, where the Rouse model is valid, this relaxation time corresponds to approximately 1/3 of the Rouse time, since the Rouse model gives $\tau_s = \Psi_{1,0}/(2\eta_0) = \eta_0 J_e^{(0)} = \pi^2 \tau_R/30$ where $J_e^{(0)}$ is the steady state compliance [20,24]. The cumulative integral of the Coleman-Markovitz equation shown in Fig. 2 extends to 800 reduced time units, which is approximately 35 shear relaxation times. Also note that our equilibration time for establishment of equilibrium and nonequilibrium steady states was 20 000 reduced time units, which is far greater than the shear relaxation time or the Rouse time. If convergence is possible, then it may lie far beyond the computing resources available to this study, even for this simple, short chain model polymer solution.

The benefit of calculating the first normal stress coefficient using Poiseuille flow is two-fold. First, one can ensure that the fluid behaves as naturally as possible by thermostating the walls instead of the fluid. Second, the time taken to obtain a reasonable value for the first normal stress coefficient is much lower in this case than in the case of evaluating the Coleman-Markovitz expression in equilibrium. This method is the equivalent of evaluating the normal stress difference at many different local strain-rates and automatically extrapolating to the zero-shear rate limit via exclusion of any nonlinear terms.

For longer polymer chains, the equilibrium method will not only be more computationally difficult, due to the bigger polymer molecules, and the larger system that it necessitates, but it will also require significantly more delay time for the correlation function to decay. The Poiseuille flow method will also suffer from the same molecule- and system-size concerns, but will benefit from the normal stress difference having a larger magnitude of response to the shear rate, generating normal stress difference profiles that are easier to resolve.

We expect that the Poiseuille flow method, in concert and mutual verification with the SLLOD method, will be very useful for obtaining the first normal stress coefficient in simulations of large polymer chain solutions and melts. As we have shown, excellent results can be obtained, but care must be taken to either stay in the linear flow regime, or to carefully extract the linear components from the data.

IV. CONCLUSION

We performed equilibrium, SLLOD, and Poiseuille flow simulations of a model polymer solution and calculated the first normal stress coefficient, $\Psi_{1,0}$, using three different methods.

The first method was to evaluate it by integrating the Coleman-Markovitz equation using the first moment of the stress autocorrelation function obtained from a homogeneous equilibrium simulation with very long averaging time. The Coleman-Markovitz equation is commonly used throughout experimental rheology, but only rarely in computer simulations, because evaluating the first moment of the computed stress autocorrelation function is extremely difficult for slowly relaxing systems like the polymer solution studied here. Our results reflect the difficulty of evaluating the Coleman-Markovitz equation, but also bring into question its validity and utility for use in molecular simulations.

The second method we used is a common alternative to the Coleman-Markovitz equation. This method uses the SLLOD equations of motion to produce homogeneous shear flow in a nonequilibrium simulation. The steady state normal pressure differences are calculated for each strain rate, and the first normal stress coefficient is calculated as a function of the strain rate, and extrapolated to zero to obtain the zero-shear first normal stress coefficient. Since SLLOD is

a nonequilibrium method in which work is done on the system, the fluid must be thermostatted to maintain a steady state.

It was previously suggested by Davis *et al.* [5] that some synthetic thermostats used in homogeneous nonequilibrium simulations of systems with periodic boundary conditions may affect $\Psi_{1,0}$. The data presented in that work showed that the first normal stress coefficient obtained from the Coleman-Markovitz equation in an equilibrium system, where the net work done by the thermostat is zero, failed to match the results obtained from SLLOD simulations, in which the work done by the thermostats was nonzero. Furthermore, the results from the SLLOD simulation varied based on the choice of thermostat. Their supposition was that the thermostat does work on the fluid of order $\dot{\gamma}^2$ and therefore may affect $\Psi_{1,0}$ which is of the same order.

However, in our work, the value of the first normal stress coefficient we obtained with the synthetically thermostatted SLLOD method agrees with the result obtained from the naturally thermostatted Poiseuille flow method, suggesting that the SLLOD method with an appropriate thermostat is indeed valid. We suggest that in the case of the atomic fluid, it is the Coleman-Markovitz value obtained by Davis *et al.* [5] that does not accurately describe the system. The small variations in their SLLOD results can be well explained by over-constraint of the kinetic degrees of freedom when all three kinetic temperatures are individually controlled, which is the only thermostat choice presented that gave results measurably different from the other SLLOD results. Such a strict constraint uniquely determines the kinetic part of the normal components of the pressure tensor [Eq. (16), for example] and leads to an unnatural pressure response and thus an incorrect $\Psi_{1,0}$. In our work, the thermostat used does not over-constrain the kinetic temperatures, and does not seem to have any effect on $\Psi_{1,0}$. This analysis is in agreement with the conclusions of Evans and Sarman [23], which indicates the equivalence of isoenergetic and isokinetic thermostatted responses under the condition that the phase variables of interest do not have trivial relationships to the chosen constants of motion.

Rigidly thermostating each configurational degree of freedom does not lead to a unique determination of the configurational component of the pressure tensor, and therefore $\Psi_{1,0}$ should be unaffected. Indeed, in the work by Davis *et al.* [5] the configurational thermostats, even those that constrain each directional configurational temperature, do not produce deviant first normal stress coefficients among the SLLOD values, which is in agreement with the analysis by Evans and Sarman [23].

Finally, we implemented a third method for calculating the first normal stress coefficient in inhomogeneous Poiseuille flow. By determining the pressure locally we can extract the local normal pressure difference, and by comparing to the local value of the strain rate, further determine the effective zero-shear rate first normal stress coefficient for the confined fluid.

In this work, only the nonequilibrium methods produce values that agree well with each other, giving a value of $\Psi_{1,0} = 170$. This suggests that the equilibrium approach using the Coleman-Markovitz equation is either only an approximation to which corrections may be needed for “fast flows” or simply profoundly difficult to exploit.

Putting validity aside, evaluating the Coleman-Markovitz integral, even for freely jointed polymer molecules with a chain length of only 20, is very difficult. Yet studies of the pressure tensor in general, and the normal stresses specifically, in microfluidic flows are important for many applications. We suspect that both the SLLOD and Poiseuille flow methods should scale well as a function of polymer chain length, compared to the Coleman-Markovitz integral. These two methods are therefore useful to calculate $\Psi_{1,0}$ in situations where the Coleman-Markovitz integral is either of uncertain validity or unable to reach convergence given the applied computational power.

We suggest that both SLLOD and Poiseuille flow methods would be well suited for calculating and verifying the first normal stress coefficient in slowly relaxing fluids, such as polymer fluids.

In future work, we plan to use nonlinear response theory [23,25] to investigate the validity of the Coleman-Markovitz equation.

ACKNOWLEDGMENTS

The computational resources for this project were provided by the National Computing Infrastructure (NCI). Adrian Menzel acknowledges the Australian Government for supporting this work through the Australian Postgraduate Award (APA).

-
- [1] X. Lu, C. Liu, G. Hu, and X. Xuan, Particle manipulations in non-Newtonian microfluidics: A review, *J. Colloid Interface Sci.* **500**, 182 (2017).
 - [2] S. M. Fielding, Vorticity structuring and velocity rolls triggered by gradient shear bands, *Phys. Rev. E* **76**, 016311 (2007).
 - [3] B. L. Holian, M. Mareschal, and R. Ravelo, Burnett-Cattaneo continuum theory for shock waves, *AIP Conf. Proc.* **1426**, 1215 (2012).
 - [4] W. G. Hoover, C. G. Hoover, and J. Petracic, Simulation of two- and three-dimensional dense-fluid shear flows via nonequilibrium molecular dynamics: Comparison of time-and-space-averaged stresses from homogeneous Doll's and Silod shear algorithms with those from boundary-driven shear, *Phys. Rev. E* **78**, 046701 (2008).
 - [5] P. J. Daivis, B. A. Dalton, and T. Morishita, Effect of kinetic and configurational thermostats on calculations of the first normal stress coefficient in nonequilibrium molecular dynamics simulations, *Phys. Rev. E* **86**, 056707 (2012).
 - [6] W. G. Hoover and C. G. Hoover, Nonlinear stresses and temperatures in transient adiabatic and shear flows via nonequilibrium molecular dynamics: Three definitions of temperature, *Phys. Rev. E* **79**, 046705 (2009).
 - [7] B. D. Coleman and H. Markovitz, Normal stress effects in second-order fluids, *J. Appl. Phys.* **35**, 1 (1964).
 - [8] B. D. Todd and P. J. Daivis, *Nonequilibrium Molecular Dynamics* (Cambridge University Press, Cambridge, 2017).
 - [9] J. D. Weeks, D. Chandler, and H. C. Andersen, Role of repulsive forces in determining the equilibrium structure of simple liquids, *J. Chem. Phys.* **54**, 5237 (1971).
 - [10] C. W. Gear, The numerical integration of ordinary differential equations, *Math. Comput.* **21**, 146 (1967).
 - [11] T. Kairn, P. J. Daivis, M. L. Matin, and I. K. Snook, Concentration dependence of viscometric properties of model short chain polymer solutions, *Polymer* **45**, 2453 (2004).
 - [12] P. J. Daivis, Thermodynamic relationships for shearing linear viscoelastic fluids, *J. Non-Newtonian Fluid Mech.* **152**, 120 (2008).
 - [13] A. G. Menzel, P. J. Daivis, and B. D. Todd, Deviations from classical hydrodynamic theory in highly confined planar Poiseuille flow of a polymer solution, *Comput. Methods Sci. Technol.* **23**, 219 (2017).
 - [14] I. K. Snook, P. J. Daivis, and T. Kairn, The flow of colloids and polymers in channels simulated using non-equilibrium molecular dynamics, *J. Phys.: Condens. Matter* **20**, 404211 (2008).
 - [15] J. Cormier, J. M. Rickman, and T. J. Delph, Stress calculation in atomistic simulations of perfect and imperfect solids, *J. Appl. Phys.* **89**, 99 (2001).
 - [16] D. M. Heyes, E. R. Smith, D. Dini, and T. A. Zaki, The equivalence between volume averaging and method of planes definitions of the pressure tensor at a plane, *J. Chem. Phys.* **135**, 024512 (2011).
 - [17] B. D. Todd, D. J. Evans, and P. J. Daivis, Pressure tensor for inhomogeneous fluids, *Phys. Rev. E* **52**, 1627 (1995).
 - [18] E. R. Smith, P. J. Daivis, and B. D. Todd, Measuring heat flux beyond Fourier's law, *J. Chem. Phys.* **150**, 064103 (2019).
 - [19] J.-P. Hansen and I. R. McDonald, *Theory of Simple Liquids*, 4th ed. (Academic Press, Oxford, 2013).
 - [20] J. D. Ferry, *Viscoelastic Properties of Polymers* (Wiley, New York, 1980).
 - [21] R. Hartkamp, P. J. Daivis, and B. D. Todd, Density dependence of the stress relaxation function of a simple fluid, *Phys. Rev. E* **87**, 032155 (2013).
 - [22] P. Prathiraja, P. J. Daivis, and I. Snook, A molecular simulation study of shear viscosity and thermal conductivity of liquid carbon disulphide, *J. Mol. Liq.* **154**, 6 (2010).

- [23] D. J. Evans and S. Sarman, Equivalence of thermostatted nonlinear responses, [Phys. Rev. E](#) **48**, 65 (1993).
- [24] M. Doi and S. F. Edwards, *The Theory of Polymer Dynamics* (Oxford University Press, Oxford, 1986).
- [25] D. J. Evans and G. P. Morriss, *Statistical Mechanics of Nonequilibrium Liquids*, 2nd ed. (Cambridge University Press, Cambridge, 2008).